BRITISH GEOLOGICAL SURVEY
TECHNICAL REPORT
Mineralogy & Petrology Series

REPORT NO. WG/99/25C

# THE MINERALOGY AND MICROTEXTURES OF SAMPLES OF THE MERCIA MUDSTONE GROUP FROM NORTHGATES, LEICESTER

S J Kemp and V L Hards

**Date**
October 27, 1999
**Classification**
Commercial-in-confidence
**Geographical index**
Northgates, Leicester, UK
**Subject index**
X-ray diffraction, scanning electron microscopy, surface area

**Bibliographic reference**
Kemp, S.J. and Hards, V.L. 1999. The mineralogy and microtextures of samples of the Mercia Mudstone Group from Northgates, Leicester
*British Geological Survey Technical Report* WG/99/25C

 British Geological Survey, Keyworth, Nottingham NG12 5GG, UK

# CONTENTS

## TABLES



## FIGURES

Page

# PLATES

## PLATES (continued)

## PLATES (continued)

**British Geological Survey**

**Mineralogy and Petrology Report No. WG/99/25C**

# THE MINERALOGY AND MICROTEXTURES OF SAMPLES OF THE MERCIA MUDSTONE GROUP FROM NORTHGATES, LEICESTER

**S J Kemp and V L Hards**

## 1. INTRODUCTION

This report presents the results of mineralogical, petrographical and surface area analyses carried out on a suite of five samples taken from the Mercia Mudstone Group. The samples were removed from boreholes drilled for the Northgates, Leicester CSO Improvements Scheme and were submitted for analysis by Mr. D. Ouston of Haswell Consulting Engineers Ltd. The client expressed a particular interest in characterizing the clay mineralogy of the samples and the identification and quantification of any 'swelling' clay minerals.

The samples, four of which were provided in plastic cartons (two per sample) while the fifth was delivered in a plastic sack, all comprise dark red-brown slurries containing fragments of mudstone, siltstone and sandstone up to 5 cm in length. Sample details are shown in Table 1.

## 2. LABORATORY METHODS

### 2. 1. General

A representative sample was removed from each sample using cone-and-quartering techniques and dried at 55°C. The dried material was then jaw-crushed to c.5 mm. A subsample of the crushed material was then hammer-milled to pass a 0.12 mm sieve for whole-rock X-ray diffraction and surface area analyses.

A further representative portion of each sample was taken for SEM analysis.

## 2. 2. X-ray diffraction analysis

### 2. 2. 1. Sample preparation

In order to provide a finer and uniform particle-size for whole-rock XRD analysis, a c.5 g portion of the hammer-milled material was wet-micronised under acetone for 10 minutes.

A c.10 g portion of the jaw-crushed material was dispersed in distilled water using a reciprocal shaker combined with treatment with ultrasound. The suspension was then sieved on 63 μm and the <63 μm material placed in a measuring cylinder and allowed to stand. In order to prevent flocculation of the clay crystals, 1 ml of 0.1M 'Calgon' (sodium hexametaphosphate) was added to each suspension. After a period dictated by Stokes' Law, a nominal <2 μm fraction was removed and dried at 55°C. 100 mg of the <2 μm material was then re-suspended in a minimum of distilled water and pipetted onto a ceramic tile in a vacuum apparatus to produce an oriented mount. The clay mounts were then Ca-saturated using 2ml 1M $CaCl_2.6H_2O$ solution and washed twice to remove excess reagent before being allowed to air-dry.

### 2. 2. 2. Analysis

XRD analysis was carried out using a Philips PW1700 series diffractometer fitted with a cobalt-target tube and operated at 45kV and 40mA. Whole-rock powders were scanned from 3-50 °2θ at 0.5 °2θ/minute. The <2 μm samples were scanned from 2-32 °2θ at 0.67 °2θ/minute as air-dry mounts, after glycol-solvation and after heating to 550°C for 2 hours. Diffraction data were analysed using Philips X'Pert software coupled to an International Centre for Diffraction Data (ICDD) database running on a Gateway personal computer system.

The XRD traces obtained from the micronised powder mounts were interpreted to give a semi-quantitative mineralogy. Appropriate standard mixtures containing the mineral phases observed were then prepared to allow production of calibration curves for comparison with experimental data. These were analysed in a similar manner and peak intensities for the main line for each of the phases present measured. These measurements were then plotted against the concentration of the phase present in the standard to produce calibration curves. The resultant mineral concentrations were then normalised to a total figure of 100 percent less the percentage smectite obtained from surface area determinations (see section 2.3. below).

2. 2. 3. XRD profile modelling

In order to gain further information about the nature of the clay minerals present in the samples, modelling of XRD profiles was carried out using Newmod-for-Windows™ (Reynolds & Reynolds, 1996) software.

Modelling was also used to assess the relative proportions of clay minerals present in the <2 μm fractions by comparison of sample XRD traces with Newmod-for-Windows™ modelled profiles. The modelling process requires the input of diffractometer, scan parameters and a quartz intensity factor (instrumental conditions) and the selection of different sheet compositions and chemistries. In addition, an estimate of the crystallite size distribution of the species may be determined by comparing peak profiles of calculated diffraction profiles with experimental data. By modelling the individual clay mineral species in this way, *mineral reference intensities* were established and used for quantitative standardization following the method outlined in Moore & Reynolds (1997).

## 2. 3. Surface area analysis

The surface area of the samples was determined using the 2-ethoxyethanol (ethylene glycol monoethyl ether, EGME) technique. The method is based on the formation of a monolayer of EGME molecules on the clay surface under vacuum. Aluminium dishes containing approximately 1.1g hammer-milled sample/clay standard (Patterson Court Blue Bentonite - the control) were firstly placed in a desiccator containing anhydrous phosphorus pentoxide, evacuated, and allowed to stand before being accurately weighed. Samples were then saturated with EGME and placed in a second desiccator containing dry calcium chloride. After one and a half hours the desiccator was evacuated and left over night. The sample was then rapidly re-weighed and the weight of the EGME absorbed determined and the surface area calculated. A correction, based on the control, was applied for slight variations between runs.

Smectite has a surface area of 800 $m^2/g$ while other clay minerals and quartz have surface areas typically less than 40 $m^2/g$ and 1 $m^2/g$ respectively. Such a difference in value means that the surface area of a sample can therefore provide a useful estimate of its smectite content.

## 2. 4. Scanning electron microscopy

### 2. 4. 1. Sample preparation

SEM examination was carried out on competent rock fragments which were carefully removed from the field moist samples, washed of clay slurry and dried. Fresh surfaces were then exposed and mounted on standard Al pin stubs using Leit-C carbon cement. These were then allowed to dry in a fume cupboard overnight. The specimens were then coated with a thin layer (~25nm thick) of carbon by evaporation in an Emitech evaporator coater to produce an electrically conductive surface to prevent charge build-up during SEM examination. Where more than one lithological type was encountered in a sample (boreholes 2/6 and 2/13), two stubs were prepared to reflect these variations.

### 2. 4. 2. Analysis

Specimens were examined in a Cambridge Instruments SEM S250 Mk 1 fitted with a Link Systems 860A energy dispersive X-ray analysis (EDXA) system which provided qualitative chemical information from areas of interest. An accelerating voltage of 20 kV was used throughout this study.

# 3. RESULTS

## 3. 1. X-ray diffraction

The results of the whole-rock XRD and surface area analyses carried out on the five Mercia Mudstone Group samples are summarised in Table 2. Labelled whole-rock XRD traces are shown in Figures 1-5.

The samples show an approximately similar mineralogy of quartz, smectite, calcite, dolomite, K-feldspar, 'mica' (undifferentiated mica species) together with traces of chlorite and hematite. Calcite forms the predominant carbonate species in the samples from boreholes 2/2, 2/6 and 2/13 whereas dolomite dominates in samples from boreholes 2/8 and 2/10. The sample from borehole 2/13, 9.05-10.30 m contains appreciably more smectite and less quartz than the other samples.

<2 μm XRD and modelling reveals some variation in the clay mineral assemblages of the samples (Table 3 and Figures 6-10). Two of the samples (boreholes 2/2 and 2/10) contain an

illite and smectite assemblage with traces of chlorite. The sample from borehole 2/13 contains a very similar assemblage with the addition of a minor sepiolite component (Newmod-for-Windows™ is unable to model such clay species and therefore no concentration has been produced). The remaining two samples have an illite and corrensite (a 50:50 trioctahedral chlorite-smectite with R=1 ordering) assemblage together with traces of chlorite.

Illite, produces a strong XRD peak at c.10Å which is ideally invariant to solvation with organic molecules or routine heat treatments. Chlorite was identified by its characteristic peak at c.14.2Å in the air-dry and ethylene glycol-solvated XRD traces. Smectite was identified on the basis of a broad $d_{001}$ air-dry peak with a spacing of c.15.5Å which expands to 16.9Å on ethylene glycol-solvation. Although minor variations in the position of the smectite peaks were noted, published tables (e.g. Moore and Reynolds, 1997) suggest that chlorite interlayering does not exceed c.5% in any of the smectite species analysed. Low-charge corrensite produces a superlattice $d_{001}$ of c.29Å in the air-dry state which expands to c.31Å in the ethylene glycol-solvated state. Rational spacings were noted in both cases. Sepiolite was identified by its characteristic peak at c.12Å which remains invariant after ethylene glycol-solvation.

In order to provide quantitative clay mineralogical data, peak integration was performed on the illite $d_{002}$ (~5Å), chlorite $d_{003}$ (4.73Å), corrensite $d_{004}$ (7.8Å) and smectite $d_{001}$ (16.9Å) reflections on the ethylene glycol-solvated traces. With the exception of the smectite $d_{001}$, these reflections are close together and therefore minimize geometry and sample thickness effects. Sample peak areas were then compared with those derived from modelling the individual clay mineral species with Newmod-for-Windows™ software, and clay concentrations produced. By measuring the 'full width at half-maximum' (FWHM) and peak intensity ratios, both species could be assigned to a 'standard' of similar crystallinity and chemistry.

## 3. 2. Scanning electron microscopy

### 3. 2. 1. Borehole 2/2, 8.00 m

This mudstone sample is predominantly composed of a fine-grained clay matrix composed of <5 μm diameter clay flakes (Plate 1). EDXA spectra indicate that the clay flakes have a K, Mg, Ca, Fe aluminium silicate chemistry in agreement with the illite, smectite and chlorite assemblage identified by XRD analysis. Small (<2 μm diameter), anhedral grains of Fe-oxide commonly occur within the matrix. Detrital silt-sized grains of quartz, albite, K-feldspar and

mica are common with rarer sand-sized, angular grains of quartz (>100 μm). Euhedral dolomite crystals and rare authigenic, 10 μm long apatite needles (up to 5 μm in diameter) were also noted (Plate 2). The matrix of clay flakes is well oriented, showing a well developed compaction lamination (Plate 3).

### 3. 2. 2. Borehole 2/6, 8.50-10.00 m

The silty-sandy mudstone clast is composed of sand-grade (up to 100 μm diameter) quartz and subangular K-feldspar (up to 50 μm diameter) grains enclosed by a fine-grained clay matrix (Plate 4). It contains abundant carbonate in the form of corroded calcite grains (up to 20 μm diameter) and small (less than 5 μm) authigenic, euhedral dolomite rhombs (Plate 5). The clay matrix comprises ragged aggregates of clay flakes which may reach 20 μm in diameter (Plate 6). EDXA spectra indicate a K, Mg, Ca, Fe aluminium silicate chemistry for the clay in agreement with the illite, corrensite and chlorite assemblage identified by XRD analysis. No discrete Fe-minerals were identified in this sample. No orientation of the clay fabric was discernable.

The clast of sandstone comprises coarse sand-grade (1 mm diameter), well-rounded quartz grains with a fine grained clay cement (Plate 7). Detrital silt-sized grains of calcite (up to 40 μm in diameter) and K-feldspar are also common. Euhedral calcite rhombs show a patchy development (Plate 8). The clay cement is formed of irregular flakes, 5-10 μm in diameter (Plate 9) and has a Mg, K, Fe, Ca aluminium silicate chemistry. Fe is probably also present as discrete oxides/oxyhydroxides, although no Fe-minerals were positively identified. The sandstone shows a high degree of porosity.

### 3. 2. 3. Borehole 2/8, 8.00 m

This sample is predominantly composed of a matrix of fine, <5 μm diameter, randomly oriented, ragged clay flakes (Plates 10 and 11). EDXA spectra again indicate a K, Ca, Mg aluminium silicate chemistry, in agreement with the illite, corrensite and chlorite and assemblage identified by XRD analysis. Iron was detected in all regions of the stub surface, and is probably present as very finely disseminated oxide or oxyhydroxides, although no iron minerals were positively identified. Detrital mineral grains include sand-grade, subangular quartz and K-feldspar (up to 100 μm in diameter) and corroded calcite (up to 40 μm diameter). Fine-grained, euhedral, authigenic dolomite crystals range up to 5 μm in diameter. The clay fabric is generally well-oriented and shows smooth, ?polished surfaces in places (Plate 12).

### 3. 2. 4. Borehole 2/10, 8.25-9.00 m

This sample is again predominantly composed of a fine-grained clay matrix composed of <10 μm diameter flakes. Again the clay has a K, Mg, Ca, Fe aluminium silicate chemistry, corresponding with the illite, smectite and chlorite assemblage identified by XRD. Detrital sand-grade (up to 100 μm) subangular K-feldspar (Plate 13) and subordinate amounts of more equant quartz are commonly observed (Plate 14). Some of the quartz grains show evidence of pitting and abrasion (Plate 15). Fine-grained (2-5 μm diameter), authigenic, euhedral dolomite is also common (Plate 15). The clay matrix shows a well developed compactional lamination.

### 3. 2. 5. Borehole 2/13, 9.05-10.30 m

The silty mudstone clast is predominantly composed of a fine-grained clay matrix with abundant silt-sized, subangular grains of quartz and K-feldspar. Euhedral dolomite and calcite crystals (up to 10 μm in diameter) are commonly developed throughout the matrix. The sample is also cross-cut by 40 μm-wide veins of fine-grained euhedral calcite crystals that reach 20 μm in diameter (Plate 16). The sample shows a high degree of porosity (Plate 17) and a lack of oriented fabric.

The mudstone clast is composed of well-oriented, <10 μm fine-grained clay flakes that bend around more competent detrital grains (Plate 18 and 20). These detrital grains include subangular quartz and K-feldspar (up to 30 μm in diameter) and corroded calcite grains of similar size (Plate 19). EDXA spectra indicate that the clay matrix has a K, Mg, Ca, Fe aluminium silicate chemistry in agreement with the illite, smectite and chlorite assemblage identified by XRD analysis. No discrete sepiolite was identified. Although Fe was detected across the stub surface, no Fe-minerals were positively identified. Fine-grained (<5 μm diameter), euhedral dolomite crystals are commonly observed within the matrix. The sample shows little porosity and a well developed compactional lamination (Plate 20).

## 4. DISCUSSION AND CONCLUSIONS

XRD analyses indicate that the samples from the Mercia Mudstone Group are composed of various proportions of the non-clay minerals quartz, calcite, dolomite, K-feldspar and hematite. Two different clay mineral assemblages were identified. The samples from boreholes 2/2 and 2/10 contain an illite and smectite assemblage with traces of chlorite while the sample from borehole 2/13 contains the same assemblage with the addition of a minor sepiolite component. The remaining samples from boreholes 2/6 and 2/8 have an illite and corrensite and minor chlorite assemblage.

Surface area analyses confirm that the five samples contain significant (>10%) proportions of the 'swelling' clay phases smectite and corrensite. Smectite-bearing Mercia Mudstone samples have also been described from an adjacent investigation for the Abbey Sewer Scheme (French *et al.*, 1998). However, standard geotechnical laboratory testing classifies such materials as having a low or intermediate plasticity. It is only after destructuring the material by mincing and the addition of water that the liquid limit begins to increase. Such an extreme degree of working might arise on a construction site during machine tunnelling, fill emplacement or bored piling (Atkinson *et al.*, 1998).

SEM analysis suggests that in general, the samples are laminated mudstones with a well-oriented clay fabric (similar to that described by Pearce *et al.*, 1996). Euhedral calcite and dolomite crystals are commonly developed. Siltstones and sandstones form a minor proportion of the lithologies represented by the samples.

Recent analyses of the clay mineralogy of the Mercia Mudstone Group in the East Midlands (e.g. Kemp, 1999; Bloodworth & Prior, 1993) suggest that the illite, smectite (or corrensite) with minor chlorite clay mineralogy of the five samples is indicative of the middle to upper parts of the group (the middle and upper Gunthorpe, Edwalton and lower Cropwell Bishop formations). The lowermost (Sneinton, Radcliffe and lowermost Gunthorpe formations) or uppermost (upper Cropwell Bishop and Blue Anchor formations) Mercia Mudstone Group is characterised by illite and chlorite clay mineral assemblages (e.g. Kemp, 1999; Hards & Kemp, 1999). The more restricted distribution of sepiolite in previous studies (e.g. Bloodworth & Prior, 1993) suggests that the five samples in this study are representative of an interval that spans the junction between the Edwalton and Cropwell Bishop formations.

## 5. REFERENCES

Atkinson, J.H., Pettifer, G.S. and Fookes, P.G. 1998. Geotechnical properties of destructured Mercia Mudstone. *CIRIA Seminar on the engineering properties of the Mercia Mudstone Group, Derby, November 1998.*

Bloodworth, A.J. and Prior, S.V. 1993. Clay mineral stratigraphy of the Mercia Mudstone Group in the Nottingham area. *British Geological Survey Technical Report* **WG/93/29**.

French, W.J., Pettifer, G.S. and Fookes, P.G. 1998. The occurrence of smectite in the Mercia Mudstone of Leicestershire. *CIRIA Seminar on the engineering properties of the Mercia Mudstone Group, Derby, November 1998.*

Hards, V.L. and Kemp, S.J. 1999. Assessment of three Mercia Mudstones for Haswell Consulting Engineers. *British Geological Survey Technical Report* **MPSR/99/58C**.

Kemp, S.J. 1999. The clay mineralogy and maturity of the Mercia Mudstone Group from the Asfordby borehole, Leicestershire. *British Geological Survey Technical Report* WG/99/7

Moore, D.M. and Reynolds, R.C. 1997. *X-Ray Diffraction and the Identification and Analysis of Clay Minerals, Second Edition.* Oxford University Press, New York.

Pearce, J.M., Kemp, S.J. and Hards, V.L. 1999. A petrographical and mineralogical study of clay minerals in the Mercia Mudstone. *British Geological Survey Technical Report* WG/96/22R.

Reynolds, R.C. and Reynolds, R.C. 1996. *Description of Newmod-for-Windows™. The calculation of one-dimensional X-ray diffraction patterns of mixed layered clay minerals.* R C Reynolds, 8 Brook Road, Hanover, NH 03755, USA.

**Table 1. Sample codes**

| Borehole | Depth (m) | BGS code |
|---|---|---|
| 2/2 | 8.00 | F241 |
| 2/6 | 8.50-10.00 | F242 |
| 2/8 | 8.00 | F243 |
| 2/10 | 8.25-9.00 | F244 |
| 2/13 | 9.05-10.30 | F245 |

**Table 2. Summary of whole-rock X-ray diffraction and surface area analyses**

| Borehole | Depth (m) | % mineral | | | | | | | | | Surface area ($m^2/g$) |
|---|---|---|---|---|---|---|---|---|---|---|---|
| | | Qtz | Calc. | Dol. | 'Mica' | K-feld | Alb. | Chl. | Hem. | Smec. | |
| 2/2 | 8.00 | 24 | 15 | 11 | 9 | 8 | 1 | 1 | 1 | 17 | 131 |
| 2/6 | 8.50-10.00 | 35 | 20 | 4 | 8 | 9 | 2 | 1 | 0 | 12 | 90 |
| 2/8 | 8.00 | 37 | 4 | 12 | 10 | 9 | 2 | 1 | 1 | 13 | 100 |
| 2/10 | 8.25-9.00 | 37 | 1 | 16 | 9 | 10 | 3 | 1 | 1 | 14 | 106 |
| 2/13 | 9.05-10.30 | 18 | 19 | 7 | 7 | 10 | 1 | 1 | 1 | 28 | 214 |

**Table 3. Summary of <2 μm X-ray diffraction analyses**

| Borehole | Depth (m) | % clay mineral | | | |
|---|---|---|---|---|---|
| | | Illite | Chlorite | Smectite | Corrensite |
| 2/2 | 8.00 | 68 | 1 | 31 | nd |
| 2/6 | 8.50-10.00 | 71 | 3 | nd | 26 |
| 2/8 | 8.00 | 66 | 3 | nd | 31 |
| 2/10 | 8.25-9.00 | 48 | 7 | 35 | nd |
| 2/13 | 9.05-10.30 | 24 | 1 | 74* | nd |

* includes minor sepiolite component

## X-RAY DIFFRACTION TRACES: KEY

Vertical axis – Intensity (counts per second)
Horizontal axis - °2θ Co-Kα

- For the whole-rock traces, only the most intense peak of each identified mineral is labelled.
- For the <2 μm traces. Black trace (air-dry), red trace (glycol-solvated) and magenta trace (heated 550°C/2 hours). Only the $d_{001}$ of each identified clay mineral is labelled on the glycol-solvated trace.

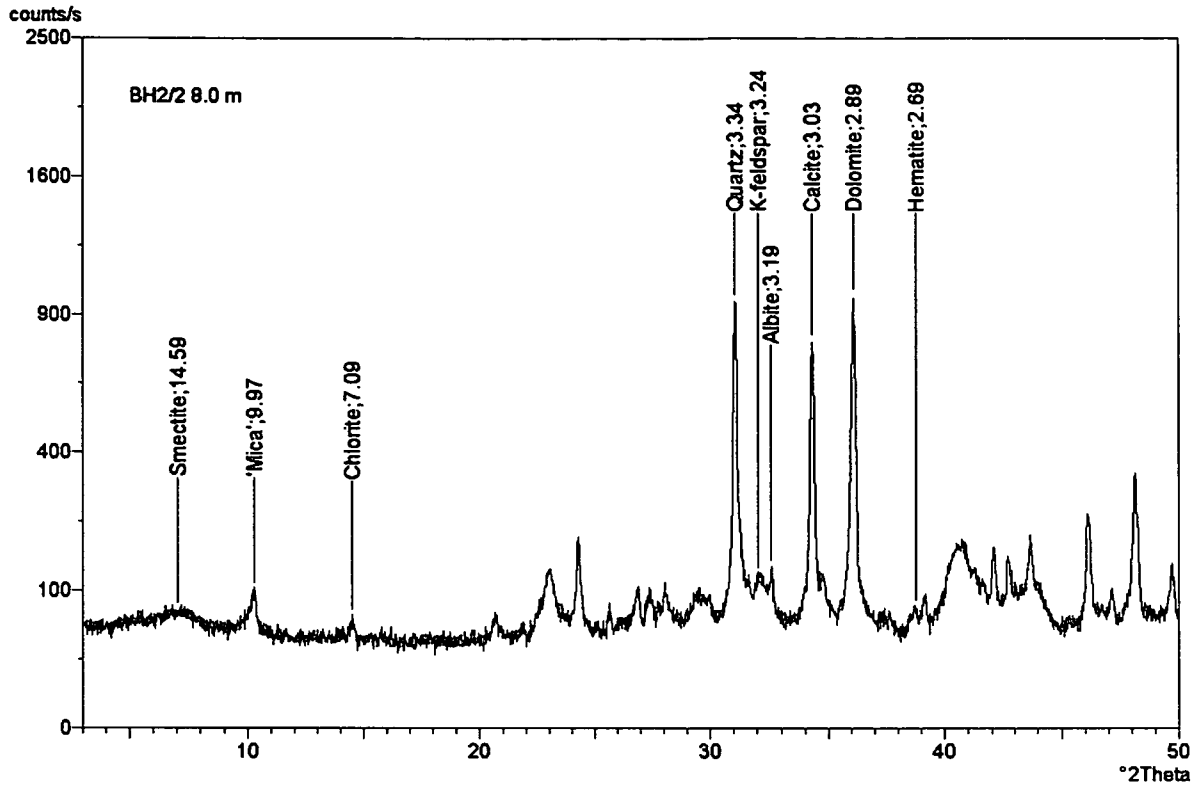


**Figure 1. Whole-rock X-ray diffraction trace, borehole 2/2, 8.00 m**

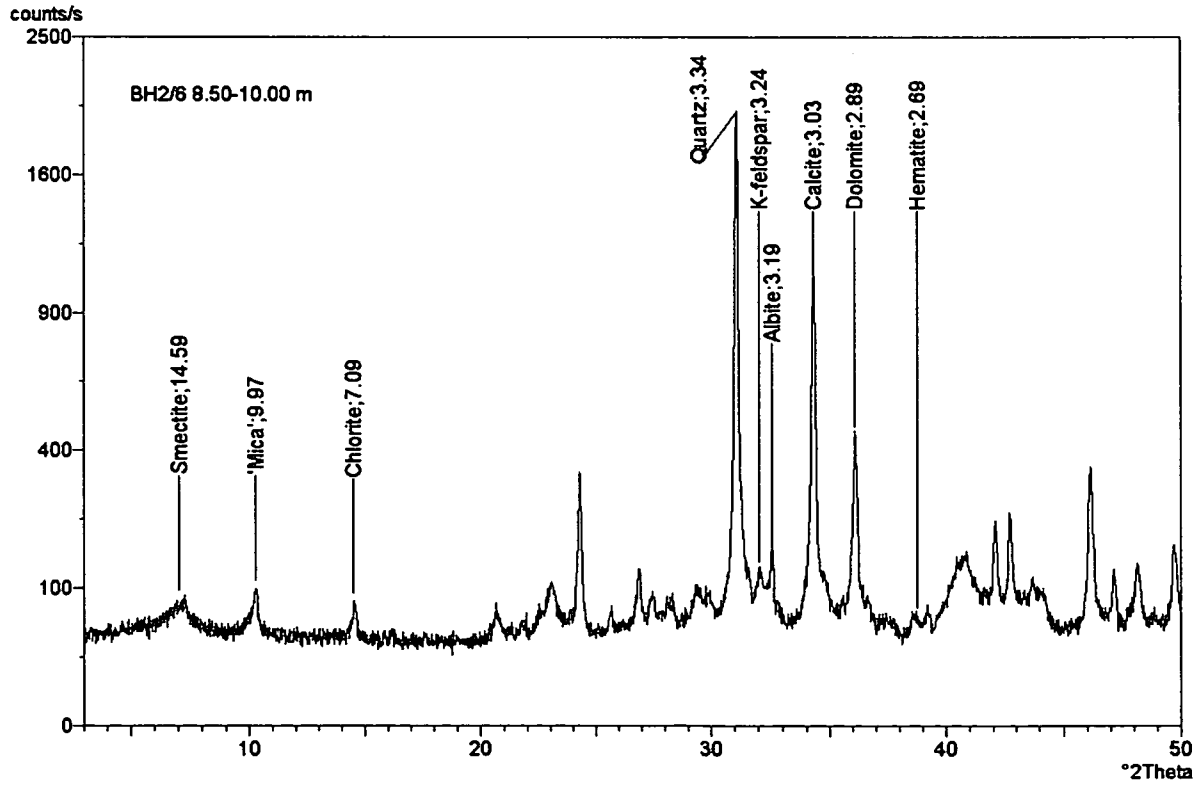


**Figure 2. Whole-rock X-ray diffraction trace, borehole 2/6, 8.50-10.00 m**

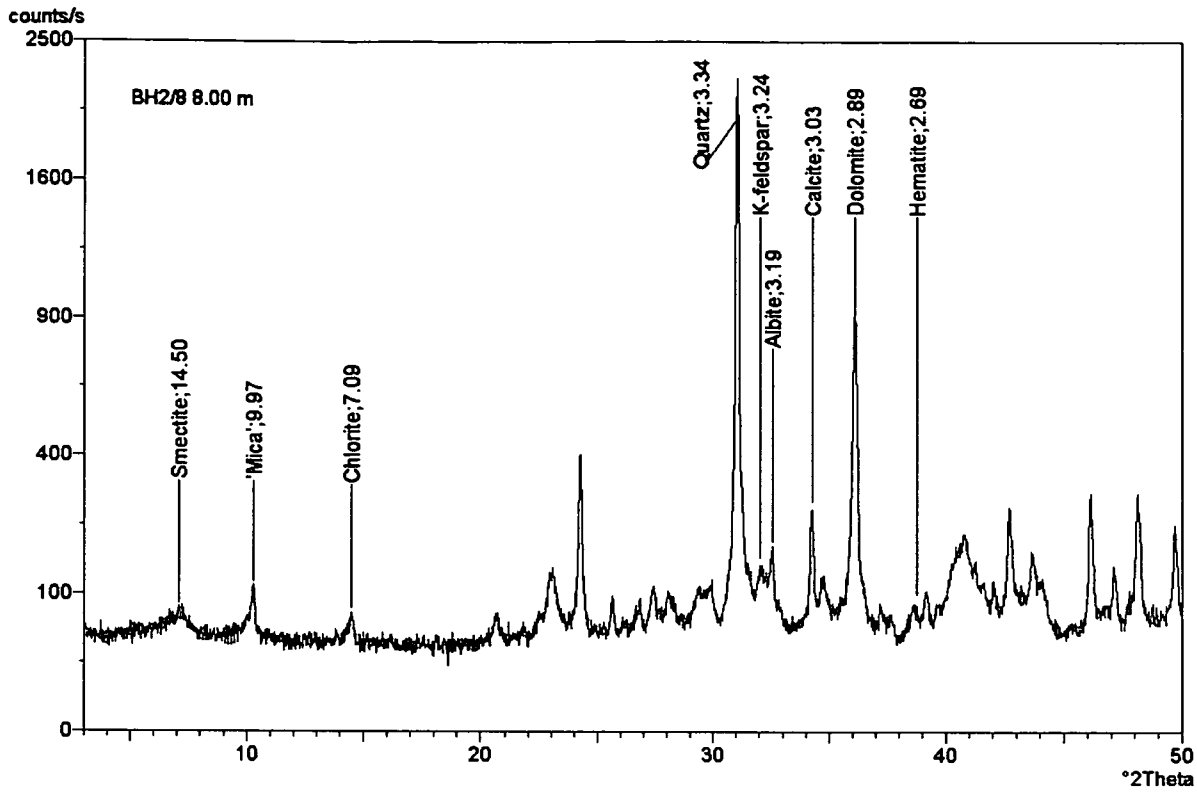


**Figure 3. Whole-rock X-ray diffraction trace, borehole 2/8, 8.00 m**

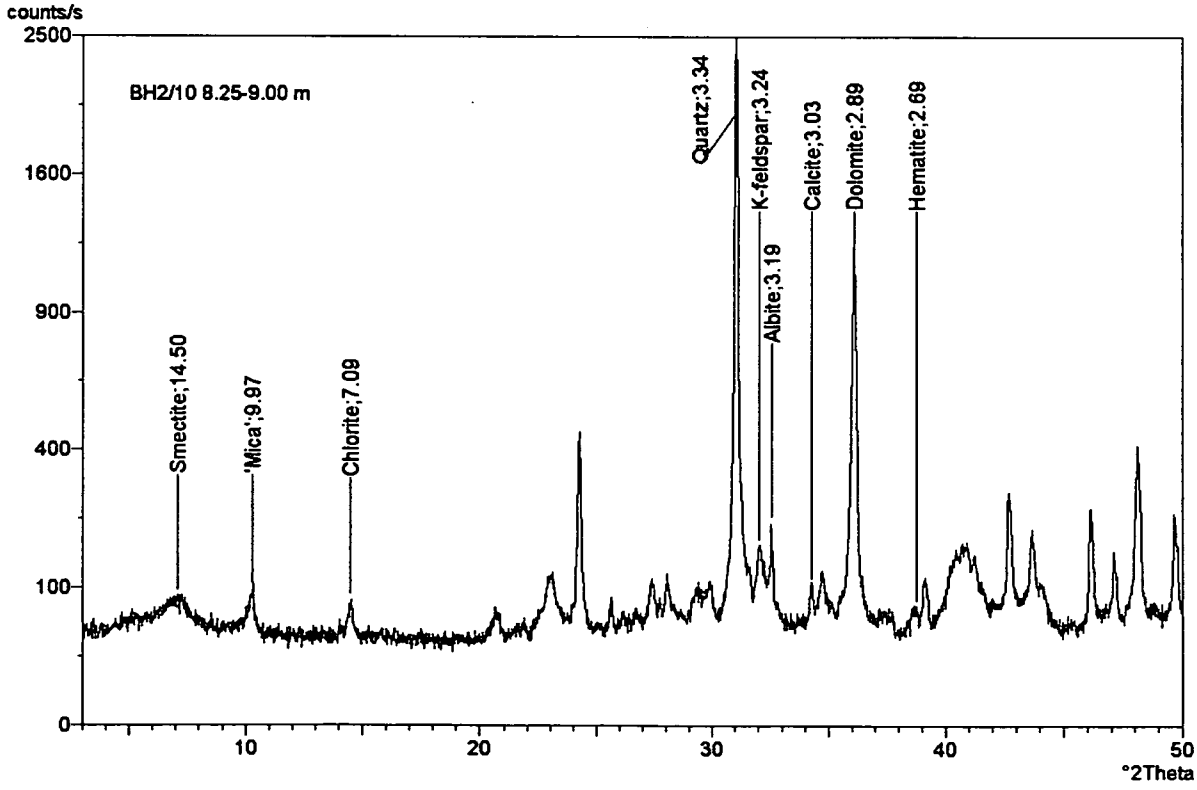


**Figure 4. Whole-rock X-ray diffraction trace, borehole 2/10, 8.25-9.00 m**

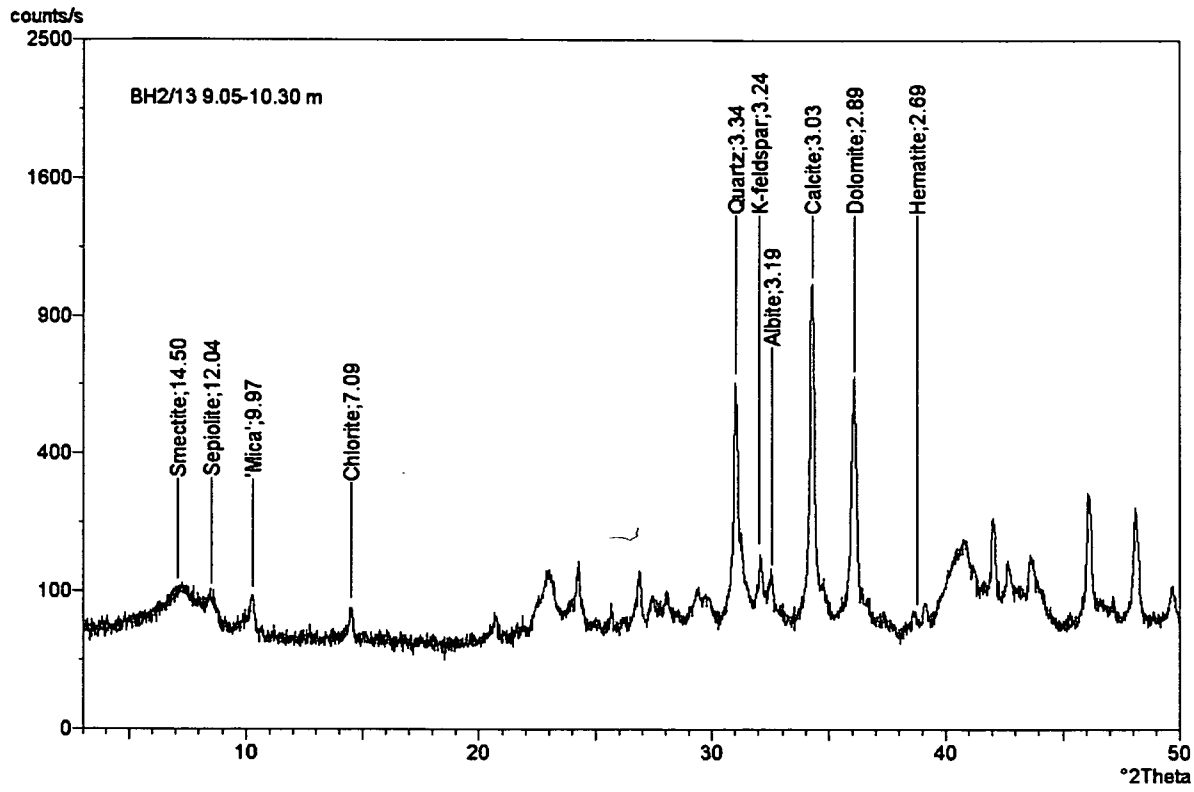


**Figure 5. Whole-rock X-ray diffraction trace, borehole 2/13, 9.05-10.30 m**

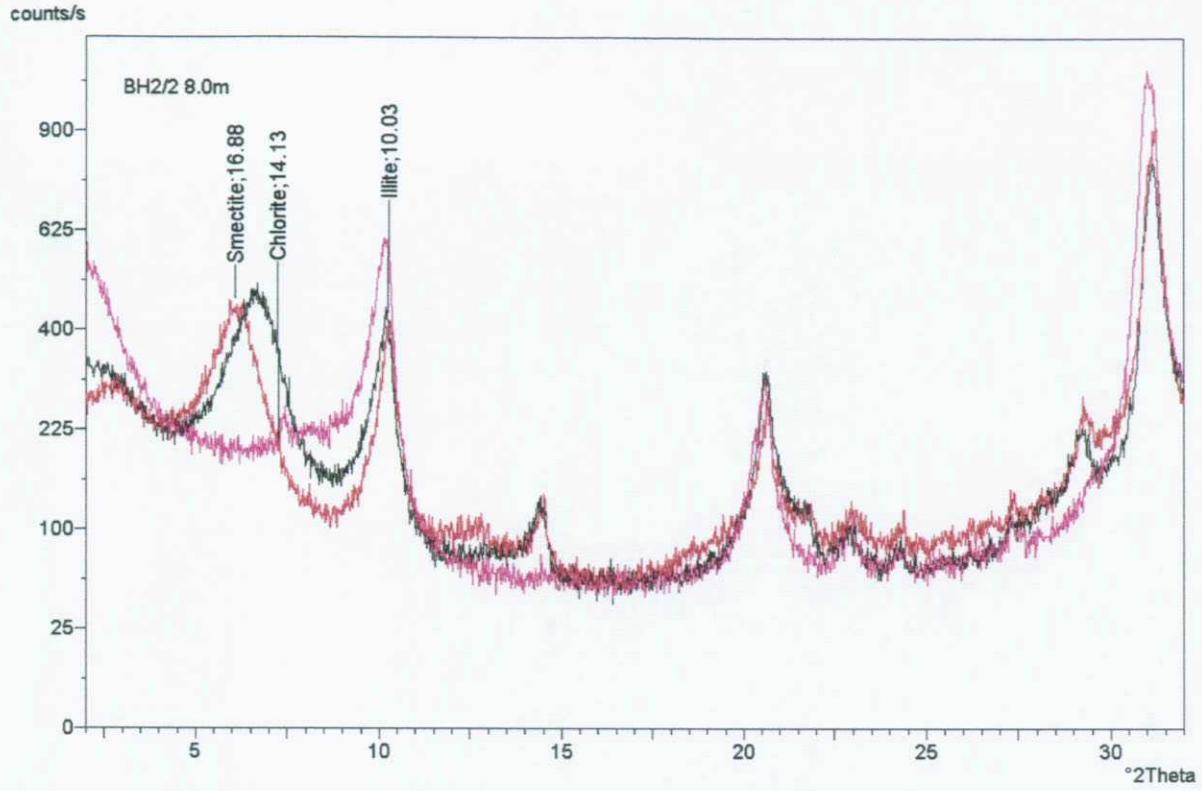


**Figure 6. <2 µm oriented mount X-ray diffraction traces, borehole 2/2, 8.00 m**

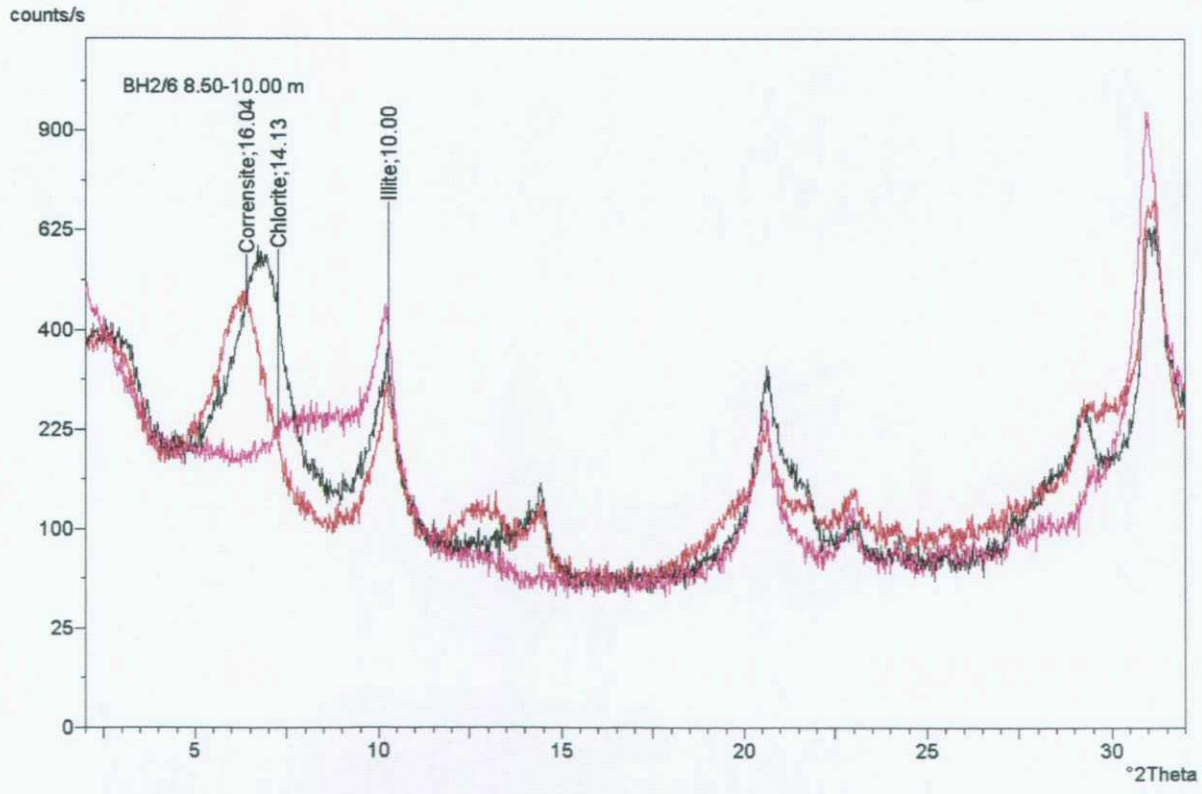


**Figure 7. <2 µm oriented mount X-ray diffraction traces, borehole 2/6, 8.50-10.00 m**

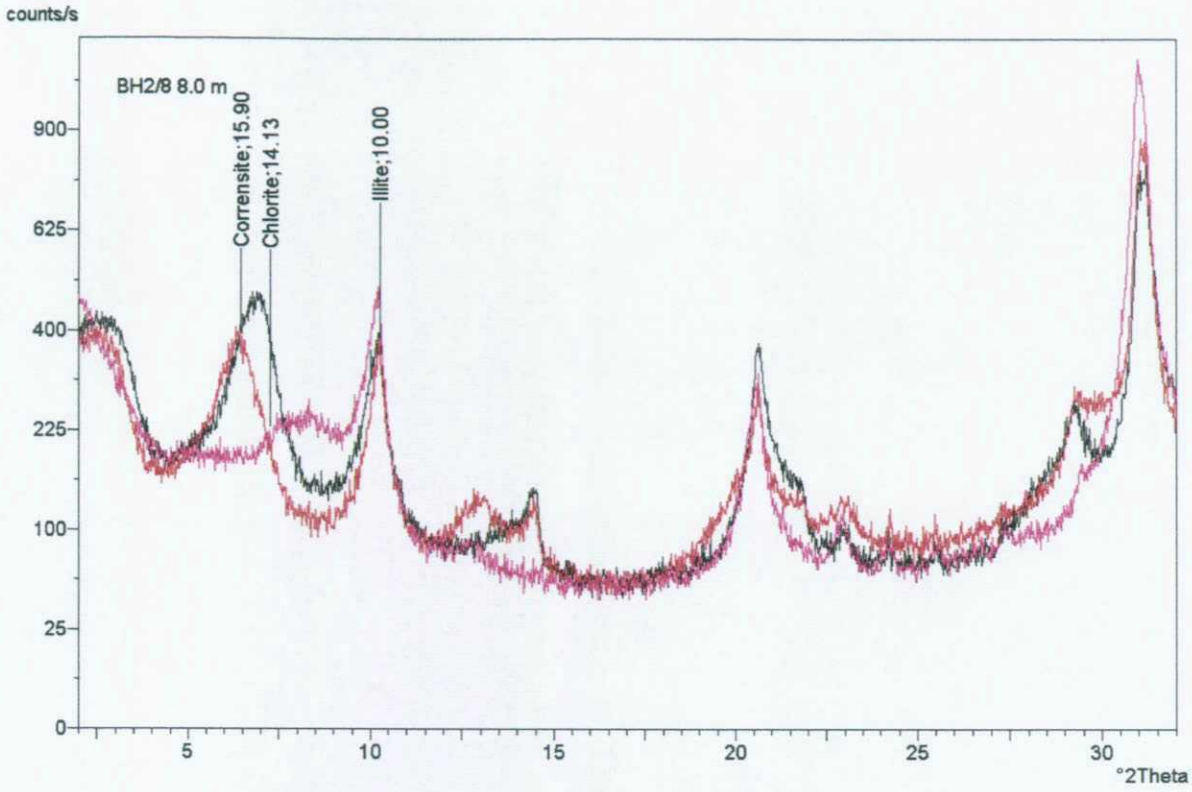


**Figure 8. <2 µm oriented mount X-ray diffraction traces, borehole 2/8, 8.00 m**

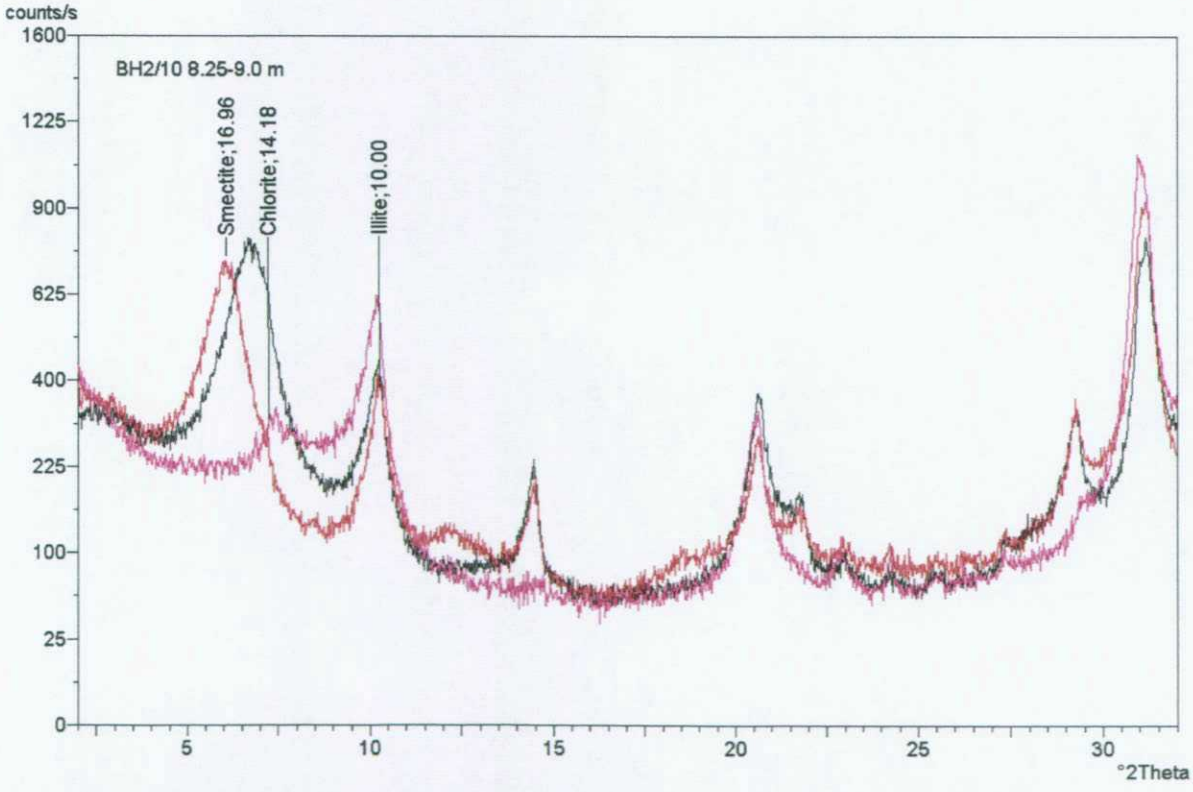


**Figure 9. <2 µm oriented mount X-ray diffraction traces, borehole 2/10, 8.25-9.00 m**

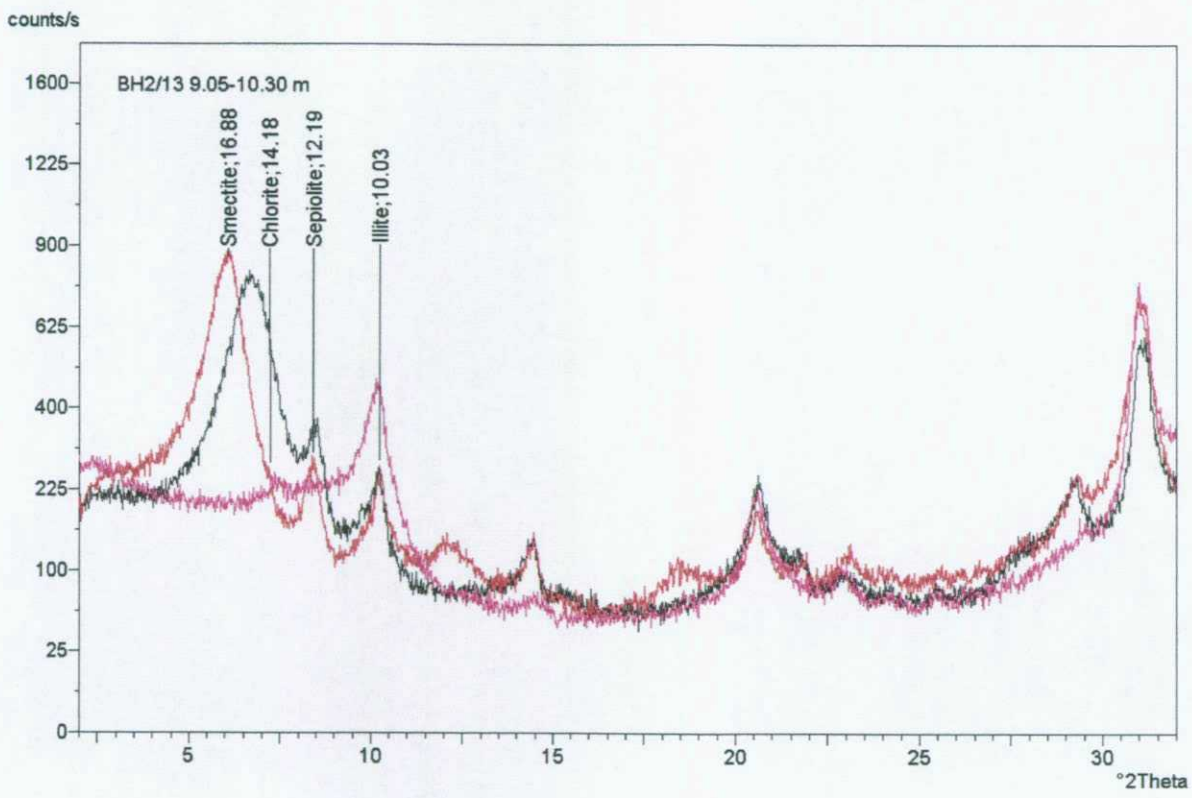


**Figure 10. <2 µm oriented mount X-ray diffraction traces, borehole 2/13, 9.05-10.30 m**

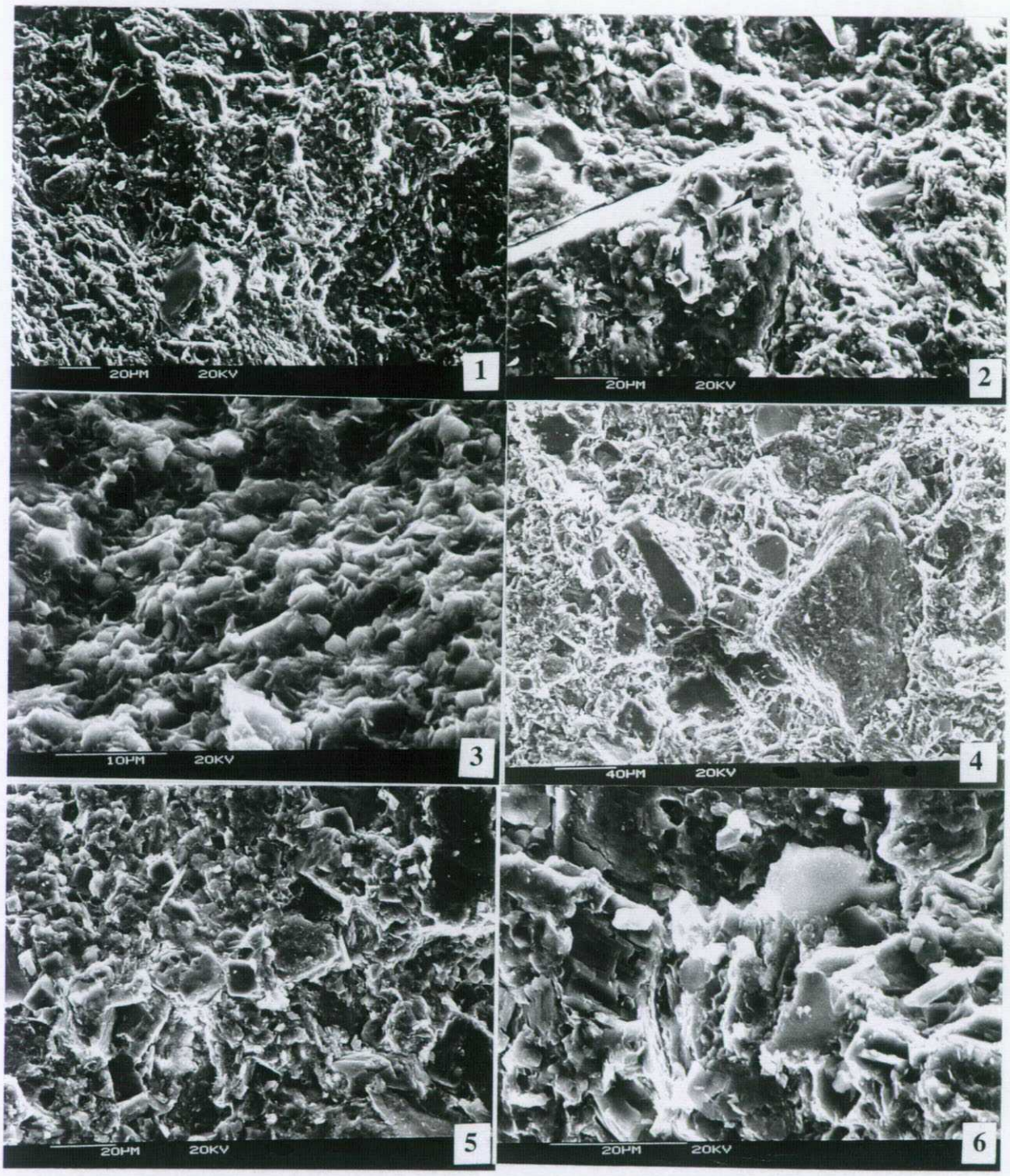


1. SEM photomicrograph showing a typical view of the fine-grained clay matrix. (Borehole 2/2 8.00 m)
2. SEM photomicrograph showing a large angular, detrital quartz grain enclosed by clay matrix. Note also the euhedral dolomite rhombs on the surface of the quartz. (Borehole 2/2 8.00 m)
3. SEM photomicrograph showing the well oriented nature of the clay fabric. (Borehole 2/2 8.00 m)
4. SEM photomicrograph showing sand-sized K-feldspar and quartz particles enclosed by clay matrix. (silty-sandy mudstone, Borehole 2/6 8.50-10.00 m)
5. SEM photomicrograph showing corroded calcite grains and authigenic, euhedral dolomite rhombs in a clay-rich matrix. (silty-sandy mudstone, Borehole 2/6 8.50-10.00 m)
6. SEM photomicrograph showing randomly oriented clay flake matrix. (silty-sandy mudstone, Borehole 2/6 8.50-10.00 m)

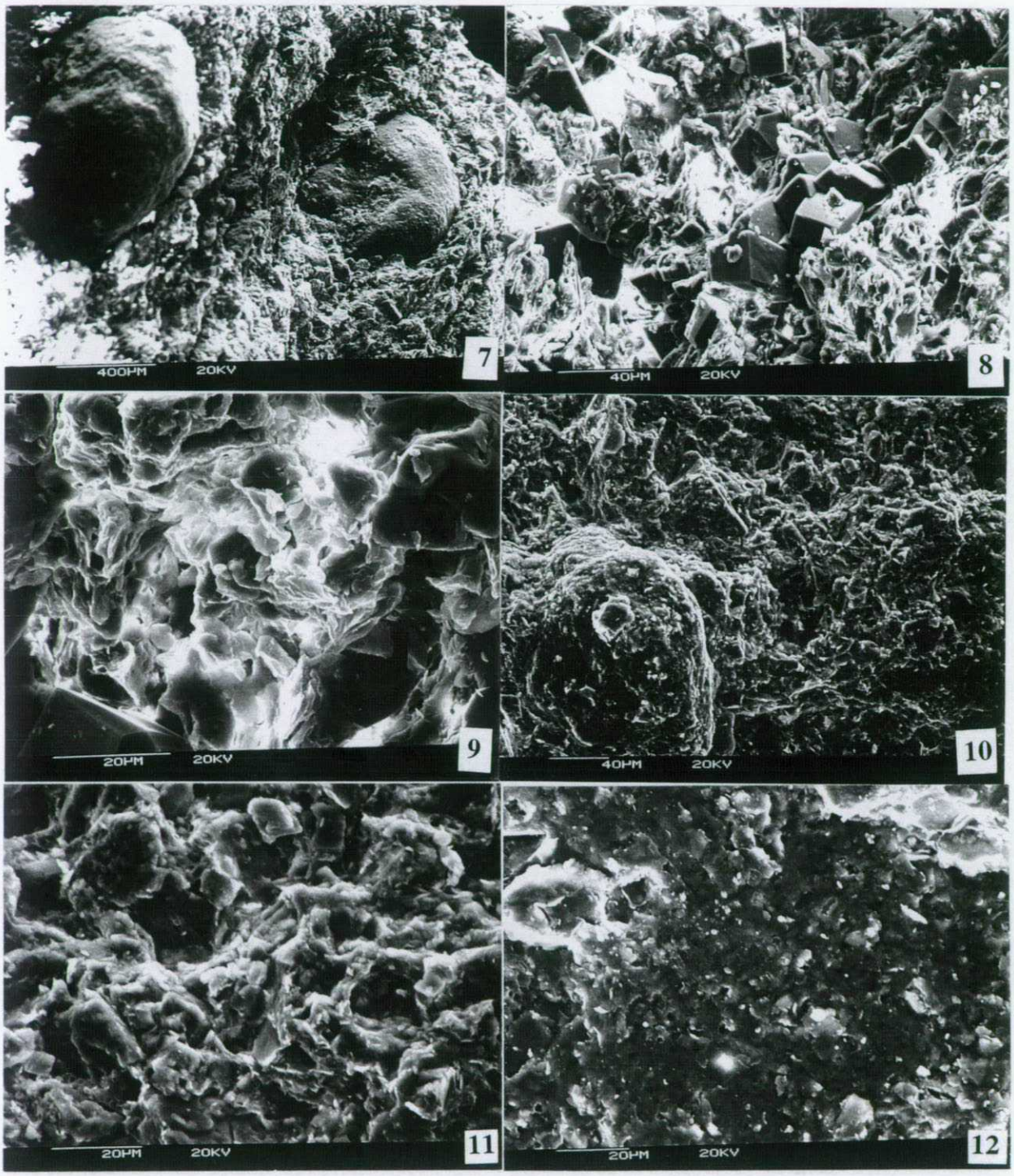


7. SEM photomicrograph showing a typical view of coarse sand grains supported by a predominantly carbonate and clay cement. (sandstone, Borehole 2/6 8.50-10.00 m)
8. SEM photomicrograph showing authigenic, euhedral calcite and dolomite rhombs and clay cement. (sandstone, Borehole 2/6 8.50-10.00 m)
9. SEM photomicrograph showing detailed view of randomly oriented clay flake cement. (sandstone, Borehole 2/6 8.50-10.00 m)
10. SEM photomicrograph showing a typical view of sand-grade quartz and feldspar grains enclosed by a fine-grained clay matrix. (Borehole 2/8 8.00 m)
11. SEM photomicrograph showing a detailed view of the randomly oriented clay flake matrix (Borehole 2/8 8.00 m)
12. SEM photomicrograph of a smooth, ?polished area of the clay matrix. (Borehole 2/8 8.00 m)

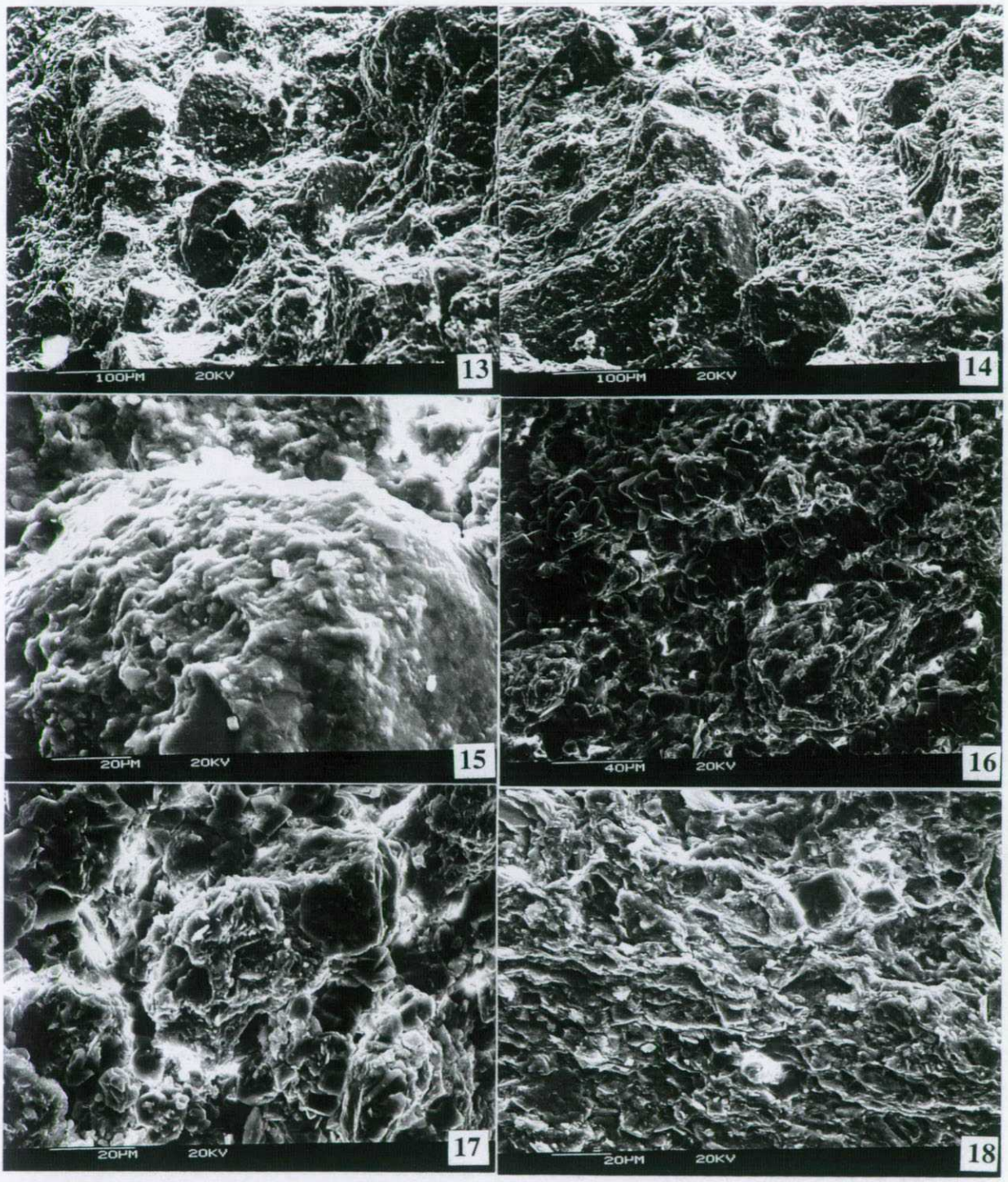


13. SEM photomicrograph of sand-sized K-feldspar grains enclosed by the clay matrix. (Borehole 2/10 8.25-9.00 m)
14. SEM photomicrograph of silt to sand sized quartz and K-feldspar grains in a laminated clay-rich matrix. (Borehole 2/10 8.25-9.00 m)
15. SEM photomicrograph showing the pitted surface of a large quartz grain with small authigenic dolomite crystals. (Borehole 2/10 8.25-9.00 m)
16. SEM photomicrograph showing the extensive development of euhedral calcite crystals in a cross-cutting vein (silty mudstone, Borehole 2/13 9.05-10.30 m)
17. SEM photomicrograph showing the highly porous nature of the silty mudstone. (silty mudstone, Borehole 2/13 9.05-10.30 m)
18. SEM photomicrograph showing the well-oriented clay flake matrix. (mudstone, Borehole 2/13 9.05-10.30 m)

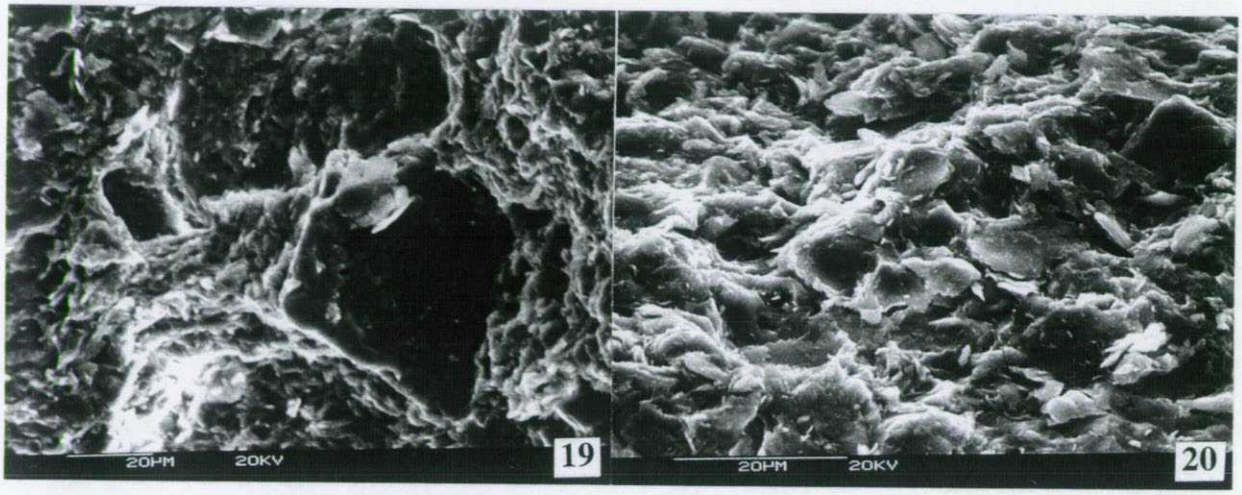


19. SEM photomicrograph showing a corroded calcite grain enclosed in clay matrix. (mudstone, Borehole 2/13 9.05-10.30 m)
20. SEM photomicrograph showing the laminated nature of the mudstone matrix. (mudstone, Borehole 2/13 9.05-10.30 m)

# BRITISH GEOLOGICAL SURVEY

# REPORT APPROVAL FORM

British Geological Survey
Kingsley Dunham Centre
Keyworth
Nottingham
United Kingdom
NG12 5GG

Tel (0115) 9363100
Fax (0115) 9363200

Report Title and Authors

**THE MINERALOGY AND MICROTEXTURES OF SAMPLES OF THE MERCIA MUDSTONE GROUP FROM NORTHGATES, LEICESTER**

**S J Kemp and V L Hards**

| Client Name and Address | Client Report No. |
|---|---|
| **Haswell Consulting Engineers Ltd**<br>**1506-1508 Coventry Road**<br>**Yardley**<br>**Birmingham**<br>**B25 8AQ** | BGS Report No. **WG/99/25C** |
| | Client Contract Ref. |
| | BGS Project Code **E83HD007** |
| | Classification **C-in-C** |

| Version | Status | Prepared by | Checked by | Approved by | Date |
|---|---|---|---|---|---|
| 1 | - | **S J Kemp** | | | 28/10/99 |
| | | | | | |
| | | | | | |